Reduced-complexity Non-data-aided Timing Recovery for PAM-based M-ary CPM Receivers

Yonggang WANG, Aijun LIU, Daoxing GUO, Xian LIU

Institute of Communication Engineering, PLA University of Science and Technology,
Yudao Street, 2, 210007, Nanjing, China

wangyg1984@163.com, Ajliu1970@163.com, Dxguo1973@163.com, liux1981@126.com

Abstract. *Continuous phase modulation (CPM) is a widely used modulation scheme in communication systems. However, difficulties arise with the design of CPM receivers, due to the nonlinear nature of CPM. One popular solution is to linearize CPM with pulse amplitude modulation (PAM) representation. In this paper, a reduced-complexity non-data-aided (NDA) timing recovery method for PAM-based M-ary CPM receivers is proposed. The proposed method is based on the PAM representation and maximum likelihood principle. The merits of the proposed method are twofold. On one hand, the proposed method is reduced-complexity in nature for PAM-based CPM receivers, i.e., it shares the match filter bank with PAM-based detectors. On the other hand, it is shown that the performance of the proposed method is better than the existing method with some modulation schemes. Therefore, the proposed method provides an important synchronization component for PAM-based M-ary CPM receivers.*

Keywords

Continuous phase modulation, pulse amplitude modulation representation, timing recovery, non-data-aided, reduced-complexity.

1. Introduction

Continuous phase modulation (CPM) is a joint bandwidth and power efficient modulation scheme with a constant envelope. It is particularly appealing in radio channels with nonlinear amplifiers, as CPM allows us to exploit the full amplifier power without any backoff. However, difficulties arise with the design of CPM receivers, due to the nonlinear nature of CPM.

One popular method of dealing with the challenges of CPM has been the pulse amplitude modulation (PAM) representation. It is a method of linearizing CPM that was first proposed for binary CPM in the well-known paper by Laurent [1]. This method has been extended to CPM in general in [2]-[5]. The PAM representation has been applied to the design of reduced-complexity detectors [6]-[11], carrier phase recovery [11], timing recovery [12]-[14], and carrier frequency recovery [15].

In this paper, we apply the PAM representation to the non-data-aided (NDA) symbol timing recovery problem for CPM signals and propose a reduced-complexity method for M-ary CPM receivers. Several NDA timing recovery methods for CPM have been proposed in previous literatures. In [12], [16]-[18], NDA methods are discussed in the context of MSK-type modulations. In [19] and [20], NDA timing recovery methods are proposed for shaped offset quadrature phase-shift keying (SOQPSK) and offset quadrature amplitude modulation (OQAM), respectively. However, all of the above methods are only suitable for one special modulation scheme, not for M-ary CPM in general. In [21], a NDA timing recovery scheme is developed for M-ary CPM in general. However, this method needs additional filters to obtain sufficient statistics for synchronization, which increases the complexity of the receivers.

In order to check out the performance of the proposed method, the method presented in [21] is employed as a comparison in analysis and simulations. Compared with the method presented in [21], the merits of the proposed method are twofold. On one hand, unlike [21] which needs additional filters, the proposed method shares the match filter (MF) bank with PAM-based reduced-complexity detectors. In other words, the proposed method is a reduced-complexity method for PAM-based CPM receivers. On the other hand, numerical results show that the proposed method is able to outperform [21] with some modulation schemes. Moreover, it is shown that the proposed method works independent of phase and can be applied to both coherent and noncoherent receivers.

The outline of the paper is structured as follows. Section 2 describes the signal model in details. In Section 3, the PAM-based maximum likelihood sequence detection (MLSD) is first reviewed. Then the proposed NDA method and corresponding digital implementation are presented. In Section 4 both analytical and numerical results are derived to evaluate the proposed method. Finally, conclusions are drawn in the Section 5.

Notation description: $E(\bullet)$ is the expectation operator. The estimated and hypothesized value of x is referred to as $\hat{x}$ and $\tilde{x}$, respectively. $(\bullet)^*$ denotes the complex conjugate, $\otimes$ denotes the convolution operation, and $\lfloor\bullet\rfloor$ denotes the floor function. $\mathrm{Re}(x)$ denotes the real part of x, $\mathrm{int}(x)$ denotes the integer part of x, and $|x|$ denotes the absolute value of x.

2. Signal Model

We introduce the conventional M-ary CPM signal model in the Subsection 2.1, and then describe the PAM-based M-ary CPM signal model in details in the Subsection 2.2.

2.1 Conventional CPM Model

The complex envelope of M-ary CPM signal is described as

$$s(t;\alpha)=\sqrt{\frac{2E_s}{T}}\exp\{j\varphi(t;\alpha)\} \tag{1}$$

where E_s is the symbol energy, T is the symbol period and $\alpha=\{\alpha_i\}$ belong to an M-ary alphabet $\{\pm1,\pm3,\cdots,\pm(\mathrm{M}-1)\}$. The phase of the signal is given by

$$\varphi(t;\alpha)=2\pi\sum_i \alpha_i h q(t-iT) \tag{2}$$

where h is the modulation index and the phase pulse $q(t)$ is the time-integral of frequency pulse with length LT and area 1/2. $L=1$ indicates that the signal is full response and $L>1$ means that the signal is partial response. In numerical examples discussed later, we consider two shapes of frequency pulse, i.e., length-LT rectangular (LREC) and length-LT raised-cosine (LRC).

2.2 PAM-based CPM Model

It was shown by Laurent [1] that the right-hand side of (1) can be formulated as a superposition of data-modulated pulses for the special case of binary (M = 2) single-h CPM. This PAM representation of CPM has been extended to M-ary CPM in [2].

Using the PAM-based model for M-ary CPM [2], we represent the complex envelope of the CPM signal as a superposition of PAM waveforms, i.e.,

$$s(t;\alpha)=\sqrt{\frac{2E_s}{T}}\sum_{m=0}^{N-1}\sum_i a_{m,i}g_m(t-iT) \tag{3}$$

where $\{a_{m,i}\}$ are the pseudo-symbols which are a nonlinear function of the real symbol sequence α, $\{g_m(t)\}$ are the PAM signal pulses. N is the number of $\{g_m(t)\}$ and $N=2^{\log_2\mathrm{M}(L-1)}(\mathrm{M}-1)$ when M is an integer power of 2. A detailed description of such pseudo-symbols can be found in [1], [2]. Similarly, the PAM pulses $\{g_m(t)\}$ are defined in [1], [2] explicitly.

An important property of PAM representation is that only a few PAM pulses count for the most energy of the signal [1], [2]. Exploiting this property, the less significant pulses can be discarded with optimal approximation technique [1], [2]. As a result, (3) turns out to be the reduced-complexity form

$$s(t;\alpha)\cong\sqrt{\frac{2E_s}{T}}\sum_{m=0}^{K-1}\sum_i a_{m,i}h_m(t-iT) \tag{4}$$

where $\{h_m(t)\}$ is the approximated PAM signal pulses, K is the number of $\{h_m(t)\}$ and $K\le N$.

3. Proposed NDA Timing Recovery Method

We briefly review the PAM-based MLSD in Subsection 3.1 and then propose the PAM-based NDA timing recovery method in Subsection 3.2. Furthermore, the corresponding digital implementation of the proposed method is presented in Subsection 3.3.

3.1 PAM-based MLSD

The signal observed at the receiver is described as

$$r(t)=s(t-\tau;\alpha)e^{j\theta}+w(t) \tag{5}$$

where $w(t)$ is the complex-valued additive white Gaussian noise with zero mean and power spectral density N_0. The variables τ and θ represent the symbol timing error and phase offset, respectively.

The symbol sequence α can be recovered using MLSD. In [7], it was shown that the likelihood function of the hypothesized symbol sequence $\tilde{\alpha}$ over the observation $0\le t\le L_0T$ is

$$\Lambda(t;\tilde{\alpha},\theta,\tau)=\mathrm{Re}[\int_0^{L_0T} r(t)s^*(t-\tau;\tilde{\alpha})e^{-j\theta}]. \tag{6}$$

Inserting (4) into (6), we derive that

$$\Lambda(t;\{\tilde{a}_{m,i}\},\theta,\tau)\cong\mathrm{Re}\{\int_0^{L_0T}[r(t)e^{-j\theta}\sum_{m=0}^{K-1}\sum_i\tilde{a}^*_{m,i}h_m(t-iT_s-\tau)]\}. \tag{7}$$

Changing the order of integration and summation, we have

$$\Lambda(t;\{\tilde{a}_{m,i}\},\theta,\tau)\cong\sum_{i=0}^{L_0-1}\mathrm{Re}[y_i(\{\tilde{a}_{m,i}\},\theta,\tau)] \tag{8}$$

which can be maximized efficiently using the Viterbi algorithm (VA). The metric increment is defined as [7]

$$y_i(\{\tilde{a}_{m,i}\},\theta,\tau)=e^{-j\theta}\sum_{m=0}^{K-1}\tilde{a}^*_{m,i}x_{m,i}(\tau) \tag{9}$$

where

$$x_{m,i}(\tau)=r(t)\otimes h_m(-t)_{|t=\tau+iT}. \tag{10}$$

Here, the time-reversed PAM pulses $\{h_m(-t)\}$ serve as the impulse response of MF bank and $x_{m,i}(\tau)$ are the outputs of MF bank sampled at the time $\tau + iT$.

3.2 Proposed PAM-based NDA Timing Recovery Method

In this subsection, we are going to derive the proposed PAM-based NDA timing recovery method. Now we assume that the timing error and phase offset are unknown. Consequently, (7) turns out to be

$$\Lambda(t;\{\tilde{a}_{m,i}\},\tilde{\theta},\tilde{\tau}) = \mathrm{Re}[\sum_{i=0}^{L_0-1} e^{-j\tilde{\theta}} \sum_{m=0}^{K-1} \tilde{a}^*_{m,i} x_{m,i}(\tilde{\tau})]. \quad (11)$$

Averaging the likelihood function with respect to θ, we have

$$\Lambda(t;\{\tilde{a}_{m,i}\},\tilde{\tau}) \cong I_0\left[\sqrt{\frac{2E_s}{T}}\frac{1}{N_0}\left|\sum_{m=0}^{K-1}\sum_{i=0}^{L_0-1}\tilde{a}^*_{m,i}x_{m,i}(\tilde{\tau})\right|\right] \quad (12)$$

where I_0 is the modified zero-order Bessel function. Here we assume a low signal to noise ratio and make the approximation, i.e., $I_0(\lambda) \cong 1+\lambda^2/4$ [21]. As a result, (12) turns out to be

$$\Lambda(t;\{\tilde{a}_{m,i}\},\tilde{\tau}) \cong \left|\sum_{m=0}^{K-1}\sum_{i=0}^{L_0-1}\tilde{a}^*_{m,i}x_{m,i}(\tilde{\tau})\right|^2. \quad (13)$$

Equation (13) can be rearranged in the following form

$$\Lambda(t;\{\tilde{a}_{m,i}\},\tilde{\tau}) = \sum_{i=0}^{L_0-1}\sum_{m_1=0}^{K-1}\sum_{m_2=0}^{K-1}\sum_{p=-i}^{L_0-1-i}\tilde{a}^*_{m_1,i}\tilde{a}_{m_2,i+p}x_{m_1,i}(\tilde{\tau})x^*_{m_2,i+p}(\tilde{\tau}). \quad (14)$$

Averaging the likelihood function with respect to $\{a_{m,i}\}$, we have

$$\Lambda(t;\tilde{\tau}) = \sum_{i=0}^{L_0-1}\sum_{m_1=0}^{K-1}\sum_{m_2=0}^{K-1}\sum_{p=-i}^{L_0-1-i}A_{m_1,m_2}(p)x_{m_1,i}(\tilde{\tau})x^*_{m_2,i+p}(\tilde{\tau}) \quad (15)$$

where $A_{m_1,m_2}(p) = E\{a^*_{m_1,i}a_{m_2,i+p}\}$ are the autocorrelations of the pseudo-symbols. The expression and property of these autocorrelation functions are well-known and the interested reader can refer to [1], [2] for details. Particularly, it is shown that absolute value of the autocorrelation functions is a decreasing function of $|p|$ [1], [2]. This property enables us to further reduce the complexity of the proposed method by truncating the likelihood function with respect to p. Consequently, (15) turns out to be

$$\Lambda(t;\tilde{\tau}) \cong \sum_{i=0}^{L_0-1}\sum_{m_1=0}^{K-1}\sum_{m_2=0}^{K-1}\sum_{p=-d}^{d}A_{m_1,m_2}(p)x_{m_1,i}(\tilde{\tau})x^*_{m_2,i+p}(\tilde{\tau}) \quad (16)$$

where d is a design parameter. We can infer that the performance of the proposed method will improve as d increases. This inference is further verified in Section 4.

Now we look for the value of τ. We define $\dot{\Lambda}(t;\tilde{\tau})$ as the derivative of $\Lambda(t;\tilde{\tau})$ with respect to τ. Then this problem can be solved by forcing $\dot{\Lambda}(t;\tilde{\tau})$ to zero. It is shown that

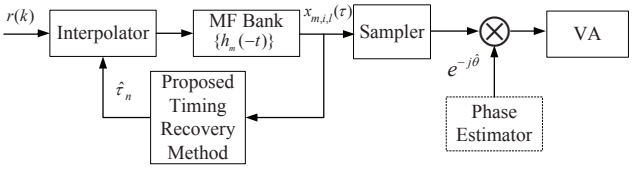

Fig. 1. Digital implementation of the proposed PAM-based NDA timing recovery system.

$$\dot{\Lambda}(t;\tilde{\tau}) \cong 2\mathrm{Re}\{\sum_{i=0}^{L_0-1}\sum_{m_1=0}^{K-1}\sum_{m_2=0}^{K-1}\sum_{p=-d}^{d}A_{m_1,m_2}(p)x_{m_1,i}(\tilde{\tau})\dot{x}^*_{m_2,i+p}(\tilde{\tau})\} \quad (17)$$

where $\dot{x}_{m,i}(\tilde{\tau})$ is the time derivation of $x_{m,i}(\tilde{\tau})$ sampled at the time $\tilde{\tau}+iT$. A discrete-time differential is used to implement $\dot{x}_{m,i}(\tilde{\tau})$, which will be discussed in the next subsection.

Then, the value of τ can be estimated in a recursive manner every L_0T.

$$\hat{\tau}_{n+1} = \hat{\tau}_n - \gamma e_n \quad (18)$$

where $\hat{\tau}_n$ is the n-th estimation of τ, e_n is the n-th error signal. γ represents the step size of the first order phase lock loop (PLL), which can be derived from the following expressions

$$\gamma = \frac{1}{E(\frac{\partial\dot{\Lambda}(t;\tau)}{\partial\tau}|\hat{\tau}=\tau)}. \quad (19)$$

3.3 Digital Implementation

Fig. 1 shows a digital implementation of the proposed method. First, the discrete signal $r(k)$ is sampled from $r(t)$ at an oversample rate Q. A sample interpolator is used to synchronize the samples based on the most recent timing estimate $\hat{\tau}_n$. Then the synchronized samples are fed to the MF bank. The output of MF bank are denoted as $x_{m,i,l}(\tau)$, where $i = \mathrm{int}(k/Q)$ and $l = k\mathrm{mod}-Q$.

In order to generate the error signals, we need to obtain $x_{m,i}(\tau)$ and $\dot{x}_{m,i}(\tau)$. Notice that $x_{m,i}(\tau)$ can be obtained by a proper combination of $x_{m,i,l}(\tau)$, and $\dot{x}_{m,i}(\tau)$ can be obtained by a proper combination of $\dot{x}_{m,i,l}(\tau)$, where $\dot{x}_{m,i,l}(\tau)$ is the time derivation of $x_{m,i,l}(\tau)$ [22], i.e.,

$$\dot{x}_{m,i,l}(\tau) = \frac{1}{2QT}[x_{m,i,l+1}(\tau) - x_{m,i,l-1}(\tau)]. \quad (20)$$

At the same time, the MF outputs $x_{m,i,l}(\tau)$ are sampled at the symbol rate and then sent to PAM-based Viterbi algorithm (VA) [6]-[11] to obtain branch metrics.

It is worth noting that the proposed method works independent of phase recovery, which means that the proposed method can be applied to both coherent and noncoherent CPM receivers. The only difference is that a additional phase estimator is needed for the noncoherent system. Moreover, as the same MF outputs are utilized in both the proposed method and PAM-based detectors, the proposed method is reduced-complexity in nature, i.e., it does not need additional filters to obtain the statistics for synchronization when applied to the PAM-based CPM receivers.

4. Performance

In Subsection 4.1, both the analytical and simulated results of S-curves for the proposed method are derived. Furthermore, the tracking performance of the proposed method is investigated by simulation in Subsection 4.2. Finally, the computational complexity of our proposed method and the method presented in [21] are compared in Subsection 4.3.

4.1 S-curves

The S-curve is a key characteristic that establishes the loop acquisition properties. It is defined as the expected value of the error signal e_n as a function of the timing offset, i.e.

$$S(\delta) = E\{e_n|\delta\} \tag{21}$$

where the timing offset is defined as $\delta = \tau - \hat{\tau}$. The S-curves give an easy method to identify the stable lock points for the method. It is also used to calculate the step size of first order PLL.

Without loss of generality, we let $\hat{\tau} = 0$. Inserting (17) into (21) , we have

$$S(\delta) = 2\mathrm{Re}\{\sum_{i=0}^{L_0-1}\sum_{m_1=0}^{K-1}\sum_{m_2=0}^{K-1}\sum_{p=-d}^{d} A_{m_1,m_2}(p)E[x_{m_1,i}(\delta)\dot{x}^*_{m_2,i+p}(\delta)]\}. \tag{22}$$

The computation of $E[x_{m_1,i}(\delta)\dot{x}^*_{m_2,i+p}(\delta)]$ is a straightforward but awkward task. The final results can be derived as follows

$$\begin{aligned} E[x_{m_1,i}(\delta)\dot{x}^*_{m_2,i+p}(\delta)] = & \int_{n_1T}^{(n_1+D_{m_1})T}\int_{n_2T}^{(n_2+D_{m_2})T}\sum_{q_1=0}^{K-1}\sum_{q_2=0}^{K-1}\sum_{i_1=I_{11}}^{I_{12}}\sum_{i_2=I_{21}}^{I_{22}} \\ & \cdot A_{m_1,m_2}(n_1-n_2)h_{m_1}(t_1-\delta-i_1T)h_{q_1}(t_1-n_1T) \\ & \cdot h_{m_2}(t_2-\delta-i_2T)\dot{h}_{q_2}(t_2-n_2T)dt_1dt_2 \end{aligned} \tag{23}$$

with

$$I_{k1} = \lfloor (t_k-\delta)/T \rfloor - D_{q_k} + 1, k = 1,2 \tag{24}$$

and

$$I_{k2} = \lfloor (t_k-\delta)/T \rfloor, k = 1,2 \tag{25}$$

where $\dot{h}_m(t)$ is the time derivation of $h_m(t)$.

Fig. 2 and Fig. 3 present the analytical and simulated S-curves of the proposed method with two schemes, i.e., M = 2, 1REC, h = 1/2 scheme and M = 4, 2RC, h = 1/4 scheme. The parameters of the simulation are set to be $K = 1, d = 0$ for the M = 2, 1REC, h = 1/2 scheme and $K = 3, d = 1$ for the M = 4, 2RC, h = 1/4 scheme, respectively. As shown in the figures, the analytical curves confirm the numerical results accurately. Moreover, no stable false lock points exist for the proposed method in these schemes. Simulations for other modulation schemes yield similar results (not shown).

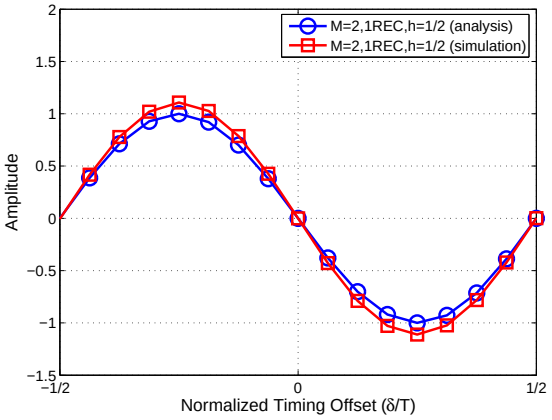

Fig. 2. S-curves for the proposed method with M = 2, 1REC, h = 1/2 scheme.

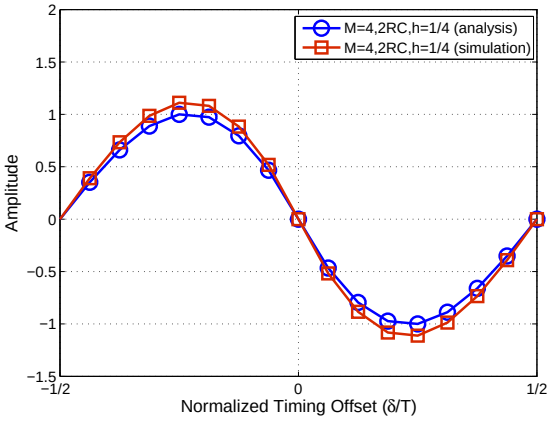

Fig. 3. S-curves for the proposed method with M = 4, 2RC, h = 1/4 scheme.

4.2 Tracking Performance

In this subsection, we will investigate the tracking performance of the proposed method. Unfortunately, no analytical method has been found to evaluate the tracking performance. Thus, we shall rely on the simulation results.

Figs. 4 - 7 present the tracking performance of the proposed method with several schemes, i.e., M = 2, h = 1/2, L = 1 schemes, M = 4, h = 1/4, L = 1 schemes, M = 2, h = 1/2, L = 2 schemes and M = 4, h = 1/4, L = 2 schemes. In order to check out the performance of the proposed method, the tracking performance of [21] and modified Cramer-Rao bound (MCRB) [21] are also shown as comparisons. In the figures the proposed method is called Prop for short, while the method presented in [21] is called Exist for short. Timing errors are normalized to the symbol period. The observation length L_0 is set to be 200 and the oversample rate Q is set to be 8. The number of PAM pulses K is set to be 1 for M = 2 schemes and 3 for M = 4 schemes, respectively. The parameter d is set to be 1 for L = 1 schemes and 3 for L = 2 schemes, respectively. It is shown that

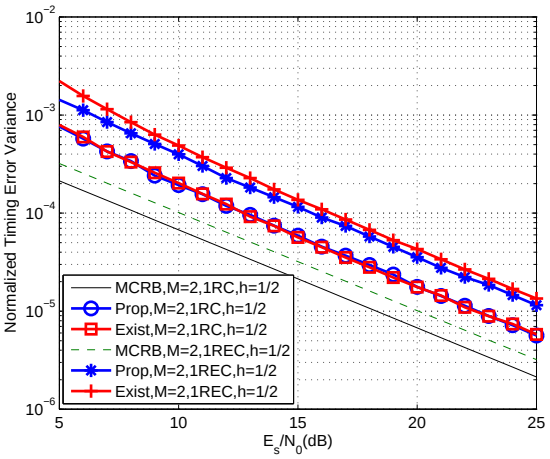

Fig. 4. Normalized timing error variance for the proposed method and method presented in [21] with M = 2, h = 1/2, L = 1 schemes.

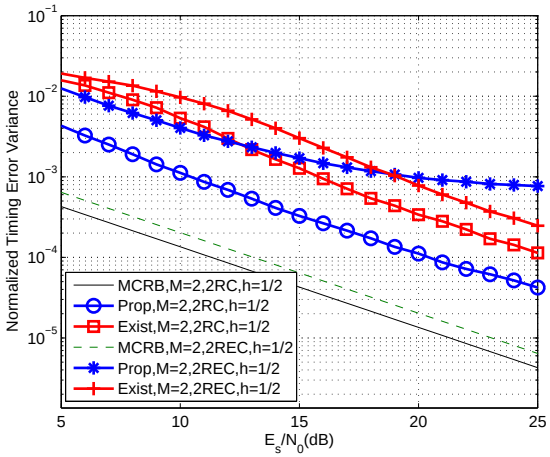

Fig. 6. Normalized timing error variance for the proposed method and method presented in [21] with M = 2, h = 1/2, L = 2 schemes.

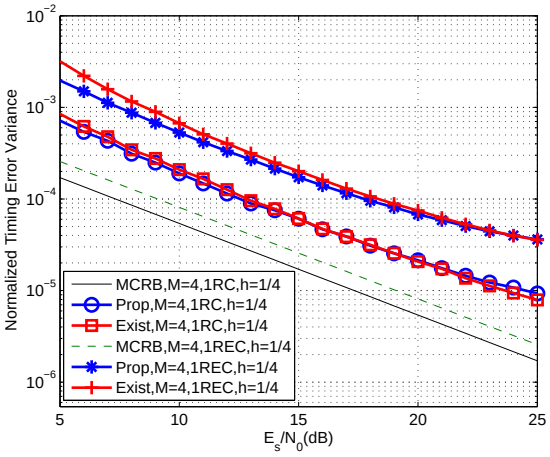

Fig. 5. Normalized timing error variance for the proposed method and method presented in [21] with M = 4, h = 1/4, L = 1 schemes.

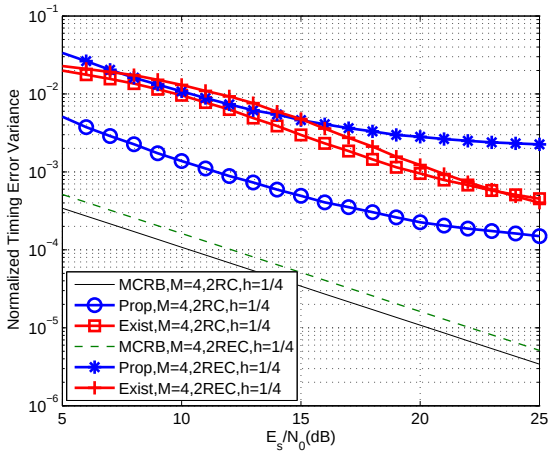

Fig. 7. Normalized timing error variance for the proposed method and method presented in [21] with M = 4, h = 1/4, L = 2 schemes.

- The performance of the proposed method is good for full response schemes, as well as the method presented in [21], but partial response schemes are more difficult to synchronize for both methods. This phenomenon can be explained as follows. During the averaging approach, NDA timing recovery methods suffer self-noises from the inter-symbol interference (ISI) of signals. Thus, limitations arise with partial response schemes with which the ISI exists.
- Similarly, the performance with LRC schemes is better than LREC schemes, due to the fact that ISI is more severe with LREC schemes than LRC schemes.
- The proposed method outperforms the method presented in [21] with some modulation schemes, e.g., M = 2, h = 1/2, 2RC scheme and M = 4, h = 1/4, 2RC scheme. Though no analytical method has been found to evaluate such phenomenon, we can give the explanation as follows. The two method average the likelihood function over data in different manners, i.e., in [21] the likelihood function is averaged over actual symbols $\{\alpha_i\}$, while it is averaged over pseudo-symbols $\{a_{m,i}\}$ in our method. As a result, the two methods suffer self-noises in different manners and it is possible that the proposed method suffers less self-noises than the one presented in [21] with some modulation schemes.

Furthermore, the effect of parameter K and d is investigated in Fig. 8. In this figure, the modulation scheme is M = 4, 2RC, h = 1/4 scheme. The observation length L_0 is set to be 100 and the oversample rate Q is set to be 8. According to the figure, we can infer that

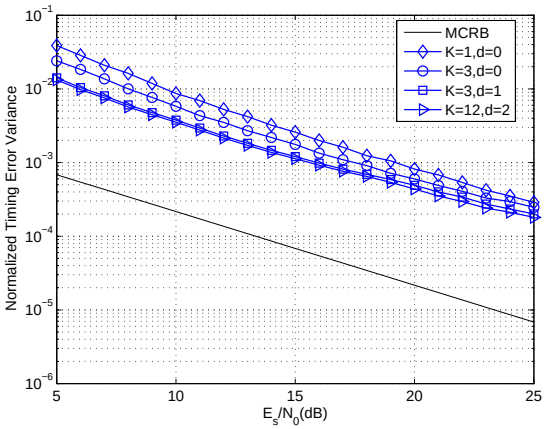

Fig. 8. Normalized timing error variance with M = 4, 2RC, h = 1/4 scheme.

Algorithm, Modulation schemes	Additions per symbol	Multiplications per symbol
Proposed Method, M = 2,L = 1 schemes	5	6
Method presented in [21], M = 2,L = 1 schemes	560	1120
Proposed Method, M = 4,L = 2 schemes	33	54
Method presented in [21], M = 4,L = 2 schemes	816	1632

Tab. 1. Computational complexity comparison between the proposed method and method presented in [21].

- The performance of the proposed method improves as the number of MFs K increases. This phenomenon corresponds to what has been found with PAM-based detectors [6]-[11] and decision-directed timing estimator [13].
- As we have expected in Subsection 3.2, the normalized timing error variance is an decreasing function of d.
- Minor improvement is seen if K and d exceed certain values. Moreover, the complexity of the proposed method increases as K and d grows. Therefore, we can infer that optimal values of K and d exist for a special modulation scheme, which minimizes the complexity while satisfactory performance is still maintained.

4.3 Computational Complexity

In Tab. 1, the computational complexity of the proposed method and the method presented in [21] are compared with several typical modulation schemes, i.e., M = 2, L = 1 schemes and M = 4, L = 2 schemes. The number of PAM pulses K is set to be 1 for M = 2 schemes and 3 for M = 4 schemes, respectively. The parameter d is set to be 1 and the oversample rate Q is set to be 8. The multiplication and additions referred are all real. In consideration of the reduced-complexity nature of the method, MFs are not taken into account when we calculate the complexity of the proposed method. As shown in the table, compared with [21], the proposed method reduces the computational complexity remarkably when applied to PAM-based CPM receivers.

5. Conclusion

In this paper, we propose a reduced-complexity NDA timing recovery method for PAM-based M-ary CPM receivers. A digital implementation of the proposed method which is easy to be realized is also presented. Compared with the existing method in [21], the proposed method is reduced-complexity in nature, due to the fact that it shares the MF bank with PAM-based CPM detectors. Furthermore, numerical results show that the performance of the proposed method is better than the existing method in [21] with some modulation schemes. Therefore, the proposed method provides an important synchronization component for the PAM-based M-ary CPM receivers.

Acknowledgements

The authors would like to thank the reviewers whose comments led to improvements to the paper.

References

[1] LAURENT, P. A. Exact and approximate construction of digital phase modulations by superposition of amplitude modulated pulses (AMP). *IEEE Transactions on Communications*, 1986, vol. 34, no. 2, p. 150 - 160.

[2] MENGALI, U., MORELLI, M. Decomposition of M-ary CPM signals into PAM waveforms. *IEEE Transactions on Information Theory*, 1995, vol. 41, no. 5, p. 1265 - 1275.

[3] PERRINS, E., RICE, M. PAM decomposition of M-ary multi-h CPM. *IEEE Transactions on Communications*, 2005, vol. 53, no. 12, p. 2065 - 2075.

[4] PERRINS, E., RICE, M. PAM representation of ternary CPM. *IEEE Transactions on Communications*, 2008, vol. 56, no. 12, p. 2020 - 2024.

[5] CARIOLARO, G., A system-theory approach to decompose CPM signals into PAM waveforms. *IEEE Transactions on Communications*, 2010, vol. 58, no. 1, p. 200 - 210.

[6] KALEH, G. K. Simple coherent receivers for partial response continuous phase modulation. *IEEE Transactions on Communications*, 1989, vol. 7, no. 12, p. 1427 - 1436.

[7] PERRINS, E., RICE, M. A new performance bound for PAM-based CPM detectors. *IEEE Transactions on Communications*, 2005, vol. 53, no. 10, p. 1688 - 1696.

[8] PERRINS, E., KUMARASWAMY, B. Decision feedback detectors for SOQPSK. *IEEE Transactions on Communications*, 2009, vol. 57, no. 8, p. 2359 - 2368.

[9] PERRINS, E., RICE, M. Reduced-complexity approach to iterative detection of coded SOQPSK. *IEEE Transactions on Communications*, 2007, vol. 55, no, 7, p. 1354 - 1362.

[10] WARDLE, M., RICE, M. PAM approach to weak CPM and its application to flight termination receivers. *IEEE Transactions on Aerospace and Electronic Systems*, 2008, vol. 44, no. 2, p. 468 - 480.

[11] COLAVOLPE, G., RAHELI, R. Reduced-complexity detection and phase synchronization of CPM signals. *IEEE Transactions on Communications*, 1997, vol. 45, no. 9, p. 1070 - 1079.

[12] MORELLI, M., VITETTA, G. M. Joint phase and timing recovery for MSK-type signals. *IEEE Transactions on Communications*, 2000, vol. 48, no. 12, p. 1997 - 1999.

[13] PERRINS, E., BOSE, S., WYLIEGREEN, M. P. Timing recovery based on PAM representation of CPM. In *IEEE Military Communications Conference, MILCOM 2008.* San Diego (CA, USA), 2008, p. 1 - 8.

[14] CHANDRAN, P., PERRINS, E. Decision-directed symbol timing recovery for SOQPSK. *IEEE Transactions on Aerospace and Electronic Systems*, 2009, vol. 45, no. 2, p. 781 - 789.

[15] D'ANDREA, A. N., GINESI, A., MENGALI, U. Frequency detectors for CPM signals. *IEEE Transactions on Communications*, 1995, vol. 43, no. 2,3,4, p. 1828 - 1837.

[16] LAMBRETTE, U., MEYR, H. Two timing recovery algorithms for MSK. In *IEEE International Conference on Communications, ICC'94*. New Orleans (USA), 1994, p. 1155 - 1159.

[17] MELHAN, R., CHEN, Y. E., MEYR, H. A fully digital feedforward MSK demodulator with joint frequency offset and symbol timing estimation for burst mode mobile radio. *IEEE Transactions on Vehicular Technology*, 1993, vol. 42, no. 4, p. 434 - 443.

[18] D'ANDREA, A. N., MENGALI, U., REGGIANNINI, R. A digital approach to clock recovery in generalized minimum shift keying. *IEEE Transactions on Vehicular Technology*, 1990, vol. 39, no. 3, p. 227 - 234.

[19] CHANDRAN, P., PERRINS, E. Symbol timing recovery for CPM with correlated data symbols. *IEEE Transactions on Communications*, 2009, vol. 57, no. 5, p. 1265 - 1270.

[20] FUSCO, T., IZZO, L., PETRELL, A., TANDA, M. Blind symbol timing estimation for OFDM/OQAM systems. *IEEE Transactions on Signal Processing*, 2009, vol. 57, no. 12, p. 4952 - 4958.

[21] D'ANDREA, A. N., MENGALI, U., MORELLI, M. Symbol timing estimation with CPM modulation. *IEEE Transactions on Communications*, 1996, vol. 44, no. 10, p. 1362 - 1372.

[22] MORELLI, M., MENGALI, U., VITETTA, G. M. Joint phase and timing recovery with CPM signals. *IEEE Transactions on Communications*, 1997, vol. 45, no. 7, p. 867 - 876.

About Authors ...

Yonggang WANG was born in Anhui, China, on January 26, 1985. He received his B.S. degree in communication engineering in 2007 from the PLA University of Science and Technology (PLAUST), Nanjing China. He is currently working toward the Ph.D. degree in satellite communication in PLAUST. His research interests include satellite communication, and digital signal processing.

Aijun LIU was born in 1970, received his Ph.D. degree from Institute of Communication Engineering in 1996. He is currently a professor at PLA University of Science and Technology. His primary research work and interests are in the area of wireless communication and signal process.

Daoxing GUO was born in 1974, received his Ph.D. degree from Institute of Communication Engineering in 2002. He is currently a professor at PLA University of Science and Technology. His research interests manly fall in the area of satellite communication, adaptive transmission and all digital receivers design.

Xian LIU was born in 1981, received his B.S. degree in communication engineering in 2003 from the PLA University of Science and Technology. He is currently working toward the Ph.D. degree in satellite communication in PLAUST. His research interests include satellite communication, and iterative receiver.